Robotics: Science and Systems 2005
Cambridge, MA, USA, June 8-11, 2005

A Two-Point Boundary-Value Approach for Planning Manipulation Tasks

Peng Song*, Vijay Kumar†, and Jong-Shi Pang‡

*Mechanical & Aerospace Engineering, Rutgers University, Piscataway, NJ 08854 Email: pengsong@jove.rutgers.edu
†GRASP Lab, University of Pennsylvania, Philadelphia, PA 19104. Email: kumar@grasp.cis.upenn.edu
‡Mathematical Sciences, Rensselaer Polytechnic Institute, Troy, NY 12180. Email: pangj@rpi.edu

***Abstract*— We consider the problem of planning manipulation tasks in which rigid body dynamics are significant and the rigid bodies undergo frictional contacts. We develop a dynamic model with frictional compliant contacts, and a time-stepping algorithm that lends itself to finding trajectories with constraints on the starting and goal conditions. Because we explicitly model the local compliance at the contact points, we can incorporate impacts without resetting the states and reinitializing the dynamic models. The problem of solving for the frictional forces with the Coulomb friction cone law reduces to a convex quadratic program. We show how this formulation can be used to solve boundary value problems that are relevant to process design, design optimization and trajectory planning with practical examples. To our knowledge, this paper is the first time boundary value problems involving changes in contact conditions have been solved in a systematic way.**

I. Introduction

There are many robotics and manufacturing processes in which nominally rigid bodies undergo frictional contacts, possibly involving impacts. Examples of such processes include robotic manipulation, part-feeding, assembly, fixturing, material handling, and disassembly. It is difficult to analyze these processes without a good understanding of the underlying dynamic model of the interaction between the multiple, nominally-rigid bodies that constitute the mechanical system [1]. Further, because these bodies undergo intermittent contacts, occasionally at significant relative velocities, it is also necessary to model the friction and, as we will shortly argue, the compliance at each contact.

Two case studies that motivate this work are (a) part-feeding; and (b) robot manipulation with multiple fingers or robots. Most current design techniques for manufacturing processes such as part-feeding are based on intuition, experience, and rules of thumb, while the analysis of designs is done empirically [2]. In contrast, there are many formal approaches to multi-robot or multi-fingered manipulation. In many cases, geometric and quasi-static models are used to successfully plan manipulation [3], [4], fixturing [5], [6], or grasping tasks [7]. However, such models are often inadequate for analysis and sometimes result in conservative motion plans (or designs) where the manipulated object must be caged [8], form-closed [9], or force-closed with guarantees on quasi-static stability [4] at all times. The use of dynamic models and design based on dynamic analysis is particularly difficult because of two main reasons. First, the use of non-smooth frictional contact models with the principles of classical rigid body dynamics introduces mathematical inconsistencies that can be hard to resolve [10]. Second, there are no accepted models for rigid body impacts. Even if we were to accept a rigid body model, it would require switching between a dynamic model with finite forces and a computation that would involve resetting the state to accommodate impacts.

Recently, there has been some attention in the robotics community on overcoming these shortcomings by using rigid body models to predict the gross motion while using compliant contact models to predict the contact forces and the local deformations [10]. Continuum models for modeling the deformations at each contact are described in [11], [12]. These models provide a better phenomenological model and also serve to regularize the problem. Existence and uniqueness can be shown for the special case of a single linearly visco-elastic frictional contact with the Coulomb friction model in two and three dimensions by Song *et al* [10]. This result has been extended to multiple frictional contacts under some restrictions on the coefficient of friction [13]. Finally, it has been shown that such compliant models yield results that converge to rigid body model results as the stiffness at the contacts is increased whenever the rigid body model predicts a unique solution [13].

Another approach to overcome the mathematical inconsistencies that are inherent in rigid body models [14] is to consider the impulse and velocity solutions instead of explicitly solving for the forces and accelerations [15], [16]. *Time-stepping methods*, which have their origins in early 80's [17], were developed to overcome some of these difficulties. The contact state (rolling, sliding or no contact) at each contact is allowed to change at any time, and the transitions between contact states are described by complementarity constraints on the relative positions (or their derivatives) and contact forces (or their integrals). Thus the process of solving for the forces and accelerations is replaced by the problem of solving for impulses and velocities at each step, which is then cast as a complementarity problem. In the special case of planar systems discretized with an explicit or a semi-implicit scheme with the Coulomb frictional contact model, the process of solving for the state at time $t^{\ell+1}$ given the state at time t^{ℓ} reduces to a linear complementarity problem (LCP), which can be solved by efficient algorithms. But more generally, a time-stepping formulation results in a nonlinear complementarity problem (NCP).

The main goal of this paper is to formulate the multi-body dynamics with compliant, frictional contacts for manipulation

tasks and develop a time-stepping model that lends itself to finding trajectories with constraints on the starting and goal conditions. Specifically, we make three important contributions in this paper. First, we build on our previous work [13] to develop a fully-implicit time stepping model incorporating compliant contacts with the Coulomb friction cone model. This requires extending the state space to model normal and tangential deformations of active contacts. Additionally, we formulate the problem of solving for the frictional forces as a convex quadratic program. Second, we formulate the trajectory design and planning problem as a boundary value problem and develop a solution technique to solve such problems. Finally, we illustrate this methodology by solving several practical examples. To our knowledge this is the first time such problems have been solved.

II. Dynamic Model

The dynamic equation of motion for a multibody system with frictional contacts can be written in the form

$$M(q)\dot{\nu} \;=\; f(t,q,\nu) + \Gamma_{\rm n}(q)^T\lambda_{\rm n} + \Gamma_{\rm t}(q)^T\lambda_{\rm t} + \Gamma_{\rm o}(q)^T\lambda_{\rm o}, \tag{1}$$

where q is the n_q-dimensional vector of generalized coordinates, ν is the n_ν-dimensional vector of the system velocities, $\dot{\nu} = d\nu/dt$, $M(q)$ is the $n_\nu \times n_\nu$ symmetric positive definite mass-inertia matrix, $f(t,q,\nu)$ is the n_ν-dimensional external force vector (excluding contact forces), and $\lambda_{\rm n,t,o}$ are the contact force vectors in the normal direction (labelled n) and the two tangential directions (labelled t and o). $\Gamma_{\rm n,t,o}$ are the Jacobian matrices defined as

$$\Gamma_{\rm n,t,o}(q) \equiv J\Psi_{\rm n,t,o}(q)G(q),$$

where $G(q)$ is a $n_q \times n_\nu$ parametrization matrix, $\Psi_{\rm n,t,o}(q)$ are the constraint functions for all possible contacts in the n, t, and o directions respectively, and $J\Psi_{\rm n,t,o}(q)$ are the corresponding Jacobian matrices of these functions. For rigid-body systems, $\lambda_{\rm n,t,o}$ are n_c-dimensional vectors, and $J\Psi_{\rm n,t,o}(q)$ are $n_c \times n_q$ matrices, where n_c is the total number of contacts. The kinematics equations relate the system velocity ν to the time-derivative of the system configuration $\dot{q} \equiv dq/dt$ via the parametrization matrix $G(q)$:

$$\dot{q} \;=\; G(q)\nu. \tag{2}$$

Together, (1) and (2) constitute the equations of motion modeling the dynamics of the mechanical system.

a) Compliant Contact Models: We employ the distributed compliant model described in [13] to model the contact forces. The key idea of the compliant model is to allow local compliance at the contact patch between nominally rigid bodies. Unlike some penalty methods, the compliant model relies on both normal and tangential compliances to model contact forces. In this paper, we adopt the simplest which postulates that the contact forces are linearly dependent on the body deformations and on the deformation rates:

$$\lambda \;=\; K(q)\delta + C(q)\dot{\delta} \tag{3}$$

where

$$\lambda \;\equiv\; \begin{pmatrix} \lambda_{\rm n} \\ \lambda_{\rm t} \\ \lambda_{\rm o} \end{pmatrix} \;=\; \lambda_{\rm n,t,o}\,, \qquad \delta \;\equiv\; \begin{pmatrix} \delta_{\rm n} \\ \delta_{\rm t} \\ \delta_{\rm o} \end{pmatrix} \;=\; \delta_{\rm n,t,o}$$

are the vector of the contact forces and the body deformations in the normal (n) and the two tangential directions (t and o), respectively; $\dot{\delta}$ denotes the vector of velocities of the deformations (i.e., $\dot{\delta} = d\delta/dt$); the stiffness matrix $K(q)$ and the damping matrix $C(q)$, which are partitioned as:

$$K(q) \;\equiv\; \begin{bmatrix} K_{\rm nn}(q) & K_{\rm nt}(q) & K_{\rm no}(q) \\ K_{\rm tn}(q) & K_{\rm tt}(q) & K_{\rm to}(q) \\ K_{\rm on}(q) & K_{\rm ot}(q) & K_{\rm oo}(q) \end{bmatrix}$$

$$\text{and} \qquad C(q) \;\equiv\; \begin{bmatrix} C_{\rm nn}(q) & C_{\rm nt}(q) & C_{\rm no}(q) \\ C_{\rm tn}(q) & C_{\rm tt}(q) & C_{\rm to}(q) \\ C_{\rm on}(q) & C_{\rm ot}(q) & C_{\rm oo}(q) \end{bmatrix}$$

are each of order $3n_s^2n_c$, with n_s^2 being the number of elements with lumped stiffness and damping properties that comprise a contact patch; each of the 18 block matrices (such as $K_{\rm nt}(q)$ etc.) in $K(q)$ and $C(q)$ is an $n_s^2n_c$ block diagonal matrix with n_c diagonal blocks, one for each contact patch, and each such diagonal block is in turn a square matrix of order n_s^2. With $n_\delta \equiv n_s^2n_c$, it follows that each of the vectors in $\lambda_{\rm n,\,t,\,o}$ and $\delta_{\rm n,\,t,\,o}$ has dimension n_δ.

b) A New Friction Model: By incorporating the compliance contact model described above with the traditional Coulomb's cone law, we can derive a new friction model that completely eliminates the discontinuities in velocities during the transitions between rolling and sliding contact states.

From Coulomb's model, the maximum power dissipation principle is formulated as

$$(\lambda_{it},\,\lambda_{io}) \;\in \underset{(\tilde{\lambda}_{it},\tilde{\lambda}_{\rm iO})\in\mathcal{FC}_i(\mu_i,\lambda_{\rm in})}{\rm argmin} \Big(s_{it}\tilde{\lambda}_{it} + s_{io}\tilde{\lambda}_{io}\Big) \tag{4}$$

where $\mu_i \geq 0$ is the friction coefficient at the ith contact and $\mathcal{FC} : \Re_+ \to \Re^2$ is the friction map at that contact, given by

$$\mathcal{FC}(\mu_i\,\lambda_{\rm in}) \;\equiv\; \left\{ (\,\lambda_{it},\lambda_{io}) \;:\; \sqrt{\lambda_{it}^2+\lambda_{io}^2} \;\leq\; \mu_i\,\lambda_{\rm in} \right\}, \tag{5}$$

and $s_{it,\rm o}$ is the tangential slip velocity given by

$$s_{it,\rm o} \;\equiv\; \dot{\delta}_{it,\rm o} + \Gamma_{it,\rm o}\nu. \tag{6}$$

Notice that the slip velocities depend on both the deformations of the compliant elements and the rigid body motions. The constitutive law (3) can be used to eliminate the slip velocities (s_{it}, s_{io}) in the friction law (4), resulting in an expression of the contact forces only in terms of the state variables (q,ν,δ). This reformulation of the friction law is significant because the slip velocities may behave discontinuously and lead to technical difficulties in the convergence of a numerical method (see [18] for a detailed discussion).

Proposition 1: Given q, ν, $\lambda_{\rm n}$, and δ, under (3), the tangential forces $(\lambda_{\rm t},\lambda_{\rm o})$ satisfy the minimum principle (4) if and

only if $(\lambda_{\rm t}, \lambda_{\rm o})$ are the optimal solution (necessarily unique) of the convex quadratic program:

$$\begin{aligned}
\text{minimize} \quad & \begin{pmatrix} \tilde{\lambda}_{\rm t} \\ \tilde{\lambda}_{\rm o} \end{pmatrix}^T \left\{ \frac{1}{2} \begin{bmatrix} \widehat{C}_{\rm tt}(q) & \widehat{C}_{\rm to}(q) \\ \widehat{C}_{\rm ot}(q) & \widehat{C}_{\rm oo}(q) \end{bmatrix} \begin{pmatrix} \tilde{\lambda}_{\rm t} \\ \tilde{\lambda}_{\rm o} \end{pmatrix} + \begin{pmatrix} d_{\rm t} \\ d_{\rm o} \end{pmatrix} \right\} \\
\text{where} \quad & \begin{pmatrix} d_{\rm t} \\ d_{\rm o} \end{pmatrix} = \begin{bmatrix} \widehat{C}_{\rm tn}(q) \\ \widehat{C}_{\rm on}(q) \end{bmatrix} \lambda_{\rm n} + \begin{bmatrix} \Gamma_{\rm t}(q) \\ \Gamma_{\rm o}(q) \end{bmatrix} \nu \\
& \qquad - \begin{bmatrix} \widehat{C}_{\rm tn}(q) & \widehat{C}_{\rm tt}(q) & \widehat{C}_{\rm to}(q) \\ \widehat{C}_{\rm on}(q) & \widehat{C}_{\rm ot}(q) & \widehat{C}_{\rm oo}(q) \end{bmatrix} K(q)\delta \\
\text{subject to} \quad & (\tilde{\lambda}_{\rm t}, \tilde{\lambda}_{\rm o}) \in \prod_{i=1}^{n_\delta} \mathcal{FC}(\mu_i \lambda_{i\rm n}) . \qquad (7)
\end{aligned}$$

Proof. From (3), we obtain

$$\dot{\delta} = C(q)^{-1}(\lambda - K(q)\delta).$$

Since

$$C(q)^{-1} \equiv \begin{bmatrix} \widehat{C}_{\rm nn}(q) & \widehat{C}_{\rm nt}(q) & \widehat{C}_{\rm no}(q) \\ \widehat{C}_{\rm tn}(q) & \widehat{C}_{\rm tt}(q) & \widehat{C}_{\rm to}(q) \\ \widehat{C}_{\rm on}(q) & \widehat{C}_{\rm ot}(q) & \widehat{C}_{\rm oo}(q) \end{bmatrix},$$

we get $\begin{pmatrix} \dot{\delta}_{i\rm t} \\ \dot{\delta}_{i\rm o} \end{pmatrix} =$

$$\begin{bmatrix} \widehat{C}_{i\rm tn}(q) & \widehat{C}_{i\rm tt}(q) & \widehat{C}_{i\rm to}(q) \\ \widehat{C}_{i\rm on}(q) & \widehat{C}_{i\rm ot}(q) & \widehat{C}_{i\rm oo}(q) \end{bmatrix} \left\{ \begin{pmatrix} \lambda_{\rm n} \\ \lambda_{\rm t} \\ \lambda_{\rm o} \end{pmatrix} - K(q)\delta \right\},$$

where $\widehat{C}_{i\rm tn}(q)$ denotes the i-th row of the (sub)matrix $\widehat{C}_{\rm tn}(q)$, and similarly for the other rows. Clearly, the friction condition (4) at contact i is equivalent to: for all $(\widetilde{\lambda}_{i\rm t}, \widetilde{\lambda}_{i\rm o}) \in \mathcal{FC}(\mu_i \lambda_{i\rm n})$,

$$\begin{aligned}
0 \;\le\; & \begin{pmatrix} \widetilde{\lambda}_{i\rm t} - \lambda_{i\rm t} \\ \widetilde{\lambda}_{i\rm t} - \lambda_{i\rm t} \end{pmatrix}^T \begin{pmatrix} s_{i\rm t} \\ s_{i\rm o} \end{pmatrix} \\
= \; & \begin{pmatrix} \widetilde{\lambda}_{i\rm t} - \lambda_{i\rm t} \\ \widetilde{\lambda}_{i\rm t} - \lambda_{i\rm t} \end{pmatrix}^T \begin{bmatrix} \widehat{C}_{i\rm tn}(q) & \widehat{C}_{i\rm tt}(q) & \widehat{C}_{i\rm to}(q) \\ \widehat{C}_{i\rm on}(q) & \widehat{C}_{i\rm ot}(q) & \widehat{C}_{i\rm oo}(q) \end{bmatrix} \cdot \\
& \left\{ \begin{pmatrix} \lambda_{\rm n} \\ \lambda_{\rm t} \\ \lambda_{\rm o} \end{pmatrix} - K(q)\delta \right\} + \begin{pmatrix} \widetilde{\lambda}_{i\rm t} - \lambda_{i\rm t} \\ \widetilde{\lambda}_{i\rm t} - \lambda_{i\rm t} \end{pmatrix}^T \begin{pmatrix} \Gamma_{i\rm t}(q) \\ \Gamma_{i\rm o}(q) \end{pmatrix} \nu .
\end{aligned}$$

This variational equation is exactly the first-order optimality conditions of the quadratic program in the proposition. □

Proposition 1 is a new result for a frictional compliant model. This quadratic program description of the tangential friction law, which we term the *friction QP*, reveals another important advantage of the compliant-body model over a rigid-body model. Namely, it follows from mathematical programming theory that the tangential forces $(\lambda_{\rm t}, \lambda_{\rm o})$ are continuous functions of the state variables (q, ν, δ) and the normal force vector $\lambda_{\rm n}$. Notice that when there are impacts, the normal force $\lambda_{\rm n}$ may still be a badly behaved function of the state variables and of time, and all contact forces remain, in general, discontinuous functions of time. It is possible, however, to overcome this by using a Hunt-Crossley type of model for impact [18].

c) Contact conditions: The contact conditions can be stated as complementarity conditions. In the normal direction,

$$0 \;\le\; \lambda_{\rm n} \;\perp\; \Psi_{\rm n}(q) + \delta_{\rm n} \;\ge\; 0, \qquad (8)$$

where the $\perp$ notation means perpendicularity and $\Psi_{\rm n}$ is the normal separation between the undeformed, contacting rigid bodies.

In the tangential direction, the contact conditions are traditionally the KKT conditions of maximum power dissipation principle (4). One of the concerns with this is that the square-root function in (5) is not differentiable at the origin, and such differentiability is essential for many numerical methods in practical computations. For our purpose, we consider a "smoothed" friction cone whereby we add a small positive scalar γ under the square root, obtaining:

$$\mathcal{FC}_\gamma(\mu_i \lambda_{i\rm n}) \equiv \left\{ (\lambda_{i\rm t}, \lambda_{i\rm o}) : \sqrt{\lambda_{i\rm t}^2 + \lambda_{i\rm o}^2 + \gamma^2} \le \mu_i \lambda_{i\rm n} + \gamma \right\}.$$

When $\gamma = 0$, the smooth cone converges to the Coulomb's quadratic cone (5). Note that the smooth cone preserves all the properties of the Coulomb's quadratic cone.

However, even for the smooth cone, there is no suitable *constraint qualification* for the KKT conditions when the contact is inactive ($\lambda_{i\rm n} = 0$) or when the contact is frictionless ($\mu_i = 0$). In practice, we use the following Fritz John conditions [19] to obtain the complementarity problem formulation for friction constraints:

$$\begin{aligned}
0 \;\le\; \beta_i \;\perp\; \mu_i \lambda_{i\rm n} + \gamma - \sqrt{\lambda_{i\rm t}^2 + \lambda_{i\rm o}^2 + \gamma^2} \;&\ge\; 0 \\
\beta_{i0} s_{i\rm t} \;+\; \frac{\beta_i \lambda_{i\rm t}}{\sqrt{\lambda_{i\rm t}^2 + \lambda_{i\rm o}^2 + \gamma^2}} \;&=\; 0 \\
\beta_{i0} s_{i\rm o} \;+\; \frac{\beta_i \lambda_{i\rm o}}{\sqrt{\lambda_{i\rm t}^2 + \lambda_{i\rm o}^2 + \gamma^2}} \;&=\; 0 \qquad (9) \\
\beta_{i0} \;\ge\; 0\,, \quad (\beta_{i0}\; \beta_i) \;&\neq\; 0
\end{aligned}$$

If $\beta_{i0} \neq 0$, the KKT conditions hold (with the Lagrange multipliers being defined as $\hat{\beta}_i \equiv \beta_i / \beta_{i0}$). In a contact problem, we can use $\mu_i \lambda_{i\rm n}$ as a natural choice for β_{i0} instead of solving for the extra multiplier. When $\mu_i \lambda_{i\rm n} = 0$, the Fritz John conditions can be trivially satisfied with a nonzero β_i. These conditions will be used in the next section to extend the traditional complementarity conditions to include impacts where inactive contacts can become active and *vice versa*.

As a practical remedy to some of the computational animosities associated with the quadratic cone, we could use a polyhedral approximation of the latter cone [20] which not only makes the complementarity conditions linear, but also automatically satisfies the constraint qualification condition.

III. Time-Stepping Methods

We partition the interval $[0, T]$ into N subintervals $[t_\ell, t_{\ell+1}]$, where $t_\ell \equiv \ell h$, for $\ell = 0, 1, \ldots, N-1$. Write

$q^\ell \equiv q(t_\ell),\ \nu^\ell \equiv \nu(t_\ell),\ \delta^\ell \equiv \delta(t_\ell),$ and $\lambda^\ell_{\rm n,t,o} \equiv \lambda_{\rm n,t,o}(t_\ell),$

replace the time derivatives ($\dot{q}$, $\dot{\delta}$, $\dot{\nu}$) with the backward Euler approximations for all $\ell = 0, \ldots, N-1$,

$$\dot{q}(t_{\ell+1}) \approx \frac{q^{\ell+1} - q^{\ell}}{h}, \quad \dot{\delta}(t_{\ell+1}) \approx \frac{\delta^{\ell+1} - \delta^{\ell}}{h},$$
$$\text{and} \quad \dot{\nu}(t_{\ell+1}) \approx \frac{\nu^{\ell+1} - \nu^{\ell}}{h},$$

together with the fully implicit discretization of the contact constraints (3, 8) and the friction QP (7) for all $i = 1 \ldots n_c$, we have the following discrete-time, mixed NCP formulation for dynamics of systems with multiple frictional contacts:

$$\begin{aligned}
&\nu^{\ell+1} = \nu^{\ell} + hM(q^{\ell+1})^{-1}u^{\ell+1} + hM(q^{\ell+1})^{-1} \ \cdot \\
&\quad \left[\, \Gamma_{\mathrm{n}}(q^{\ell+1})\lambda_{\mathrm{n}}^{\ell+1} + \Gamma_{\mathrm{t}}(q^{\ell+1})\lambda_{\mathrm{t}}^{\ell+1} + \Gamma_{\mathrm{o}}(q^{\ell+1})\lambda_{\mathrm{o}}^{\ell+1} \,\right] \\
&q^{\ell+1} = q^{\ell} + hG(q^{\ell+1})\nu^{\ell+1} \\
&0 \le \lambda_{i\mathrm{n}}^{\ell+1} \perp \Psi_{i\mathrm{n}}(q^{\ell+1}) + \delta_{i\mathrm{n}}^{\ell+1} \ge 0 \qquad (10) \\
&\left(\lambda_{i\mathrm{t}}^{\ell+1},\ \lambda_{i\mathrm{o}}^{\ell+1}\right) \in \underset{(\tilde{\lambda}_{i\mathrm{t}}, \tilde{\lambda}_{i\mathrm{o}}) \in \mathcal{FC}_i(\mu_i, \lambda_{i\mathrm{n}})}{\operatorname{argmin}} \left(\tilde{\lambda}_{i\mathrm{t}}^{\ell+1} \ \ \tilde{\lambda}_{i\mathrm{o}}^{\ell+1}\right) \cdot \\
&\left\{ \frac{1}{2} \begin{bmatrix} \widehat{C}_{\mathrm{tt}}(q^{\ell+1}) & \widehat{C}_{\mathrm{to}}(q^{\ell+1}) \\ \widehat{C}_{\mathrm{ot}}(q^{\ell+1}) & \widehat{C}_{\mathrm{oo}}(q^{\ell+1}) \end{bmatrix} \begin{pmatrix} \tilde{\lambda}_{i\mathrm{t}}^{\ell+1} \\ \tilde{\lambda}_{i\mathrm{o}}^{\ell+1} \end{pmatrix} + \begin{pmatrix} d_{i\mathrm{t}}^{\ell+1} \\ d_{i\mathrm{o}}^{\ell+1} \end{pmatrix} \right\} \\
&\lambda_{i\,\mathrm{n,t,o}}^{\ell+1} = \left(K_{i\,\mathrm{n,t,o}} + \frac{1}{h} C_{i\,\mathrm{n,t,o}} \right) \delta_{i\,\mathrm{n,t,o}}^{\ell+1} - \frac{1}{h} C_{i\,\mathrm{n,t,o}} \delta_{i\,\mathrm{n,t,o}}^{\ell}
\end{aligned}$$

where

$$d_{i\mathrm{t,o}}^{\ell+1} \equiv d_{\,i\mathrm{t,o}}(q^{\ell+1}, \nu^{\ell+1}, \delta^{\ell+1}).$$

The description of the model is complete with the stipulation of initial conditions or boundary conditions, which we prescribe as a functional equation involving the initial state (q^0, ν^0, δ^0) and the final state (q^N, ν^N, δ^N):

$$\Upsilon(q^0, \nu^0, \delta^0, q^N, \nu^N, \delta^N) \ = \ 0.$$

Solving for the above model involves the solution of nonlinear equations, because the inertia matrix and the Jacobians are functions of the unknown states $q^{\ell+1}$. Note that this *fully implicit* scheme enforces the complementarity conditions precisely at the end of each time step.

The existence of a discrete-time solution trajectory to the fully implicit time-stepping compliant model (10) can be shown for not only the initial value problem but also the boundary-value multibody contact problem under the assumption that the friction coefficients are sufficiently small. Moreover, we have shown that such a discrete-time solution trajectory converges to the weak solution of the corresponding continuous-time problem [18].

There is extensive work on solving the initial value problems using the time-stepping model with complementarity constraints [21], [20], where the solution trajectory can be obtained by stepping through the time iteratively. In each time step, a relatively small sized LCP or NCP is solved to update the states variables from the known states variables obtained at the previous time step. When impact occurs, using this method, one can stop the simulation at the time of the impact and use an impact model to reset the velocity variables, and then resume the simulation with the post-impact states. This becomes problematic when dealing with boundary value problem since model switching is no long available. For boundary value problems, we need to solve the complete trajectory as a whole by solving a large scale NCP problem consisting of model (10) at every time step $\ell = 0, \ldots, N-1$. We use the PATH solver to solve the NCP (10). The equations are first programmed into AMPL and then get passed into the PATH solver through a AMPL/PATH interface.

IV. Examples

A. Transitions between rolling and sliding

Consider the problem of dynamically feasible trajectory for a planar rolling disk in contact with a horizontal plane as depicted in Figure 1, such that the disk starts with velocities that correspond to sliding contact with a desired final state at a specified time corresponding to a specified position and rolling condition. This is the simplest example of a boundary value problem involving transitions in contact conditions, one that is seen in a freshman mechanics class. The traditional approach to solving it is in two stages (the sliding phase and then the rolling phase), using different equations for both stages, often requiring iteration to determine the time of transition between the phases. We wish to solve this problem automatically by simply specifying the end conditions.

The dynamics equation are given by (1) with

$$q = \begin{pmatrix} x \\ \theta \end{pmatrix}, \quad \nu \equiv \begin{pmatrix} v \\ \omega \end{pmatrix}, \quad \Gamma_{\mathrm{t}}(q) = \begin{pmatrix} 1 \\ r \end{pmatrix},$$
$$M(q) = \begin{bmatrix} m & 0 \\ 0 & I \end{bmatrix}, \quad G(q) = \begin{bmatrix} 1 & 0 \\ 0 & 1 \end{bmatrix},$$
$$\dot{q} = G(q)\nu, \quad f(t, q, \nu) = 0.$$

The analytical solutions of the boundary value problem can be obtained by solving an algebraic equation after the integration. For example, given other boundary conditions, the transition time τ and the initial velocity v^0 can be determined by

$$\begin{aligned}
\tau &= \frac{\omega^0 r + v^0}{\mu g (1 + \frac{mr^2}{I})}, \\
v^0 &= \left\{ v \,:\, av^2 + bv + c \,=\, 0 \right\} \ , \\
\text{where} \qquad a &= \frac{1}{2\mu g (1 + \frac{mr^2}{I})^2} \ , \\
b &= 2a\omega^0 r + T - \frac{T}{1 + \frac{mr^2}{I}} \ , \\
c &= x^0 - x^T + a(\omega^0)^2 r^2 - \frac{\omega^0 r}{1 + \frac{mr^2}{I}} \ .
\end{aligned}$$

Using the paramters, $\mu = 4$, $r = 0.1m$, $m = 0.1kg$, $I = 5e-4kg\,m^2$, and the boundary conditions $T = 0.022sec$, $x^0 = 0$, $\omega^0 = 1rad/sec$, and $x^{N+1} = 0.02m$, we get $v^0 = 1.2402m/sec$ and $\tau = 0.0114sec$.

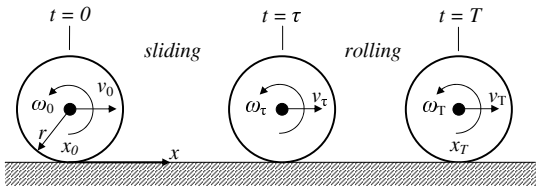

Fig. 1. A sliding/rolling disk on the horizontal plane

We now solve this problem using the time-stepping method. This example is a very special case where M, f, G, and $J\Psi$ are constant matrices, which leads to the following mixed LCP for the time-stepping formulation: for $\ell = 0, \ldots, N$,

$$0 = -\nu^{\ell+1} + \nu^{\ell} + \frac{h}{2} M^{-1} \Gamma_{\mathrm{t}}^{T} (\lambda_{\mathrm{t}+}^{\ell+1} - \lambda_{\mathrm{t}-}^{\ell+1}) \,,$$

$$0 = -q^{\ell+1} + q^{\ell} + h\nu^{\ell+1} \,,$$

$$0 = s_{\mathrm{t}+}^{\ell+1} - s_{\mathrm{t}-}^{\ell+1} - \Gamma_{\mathrm{t}} \nu^{\ell+1} \,,$$

$$0 = \lambda_{\mathrm{t}+}^{\ell+1} + \lambda_{\mathrm{t}-}^{\ell+1} - 2\mu m g \,,$$

$$0 \le \begin{pmatrix} \lambda_{\mathrm{t}+}^{\ell+1} \,, \\ s_{\mathrm{t}-}^{\ell+1} \end{pmatrix} \perp A^{\ell} \begin{pmatrix} \lambda_{\mathrm{t}+}^{\ell+1} \,, \\ s_{\mathrm{t}-}^{\ell+1} \end{pmatrix} + \begin{bmatrix} \Gamma_{\mathrm{t}} \\ 0 \end{bmatrix} \nu^{\ell} + b^{\ell} \ge 0 \,,$$

$$0 = \Upsilon(q^0, \nu^0, q^N, \nu^N)$$

$$= \begin{bmatrix} -1 & 0 & 0 & 0 & 1 & 0 & 0 & 0 \\ 0 & 0 & 0 & 1 & 0 & 0 & 0 & 0 \\ 0 & 0 & 0 & 0 & 1 & 0 & 0 & 0 \\ 0 & 0 & 0 & 0 & 0 & 0 & 1 & r \end{bmatrix} \begin{pmatrix} q^0 \\ \nu^0 \\ q^{N+1} \\ \nu^{N+1} \end{pmatrix} - \begin{pmatrix} 0.02 \\ \omega_0 \\ x_T \\ 0 \end{pmatrix} ,$$

$$A^{\ell} = \begin{bmatrix} h\,\Gamma_t M^{-1} \Gamma_{\mathrm{t}}^{T} & 1 \\ -1 & 0 \end{bmatrix} ,$$

$$b^{\ell} = \begin{pmatrix} h\,[\,\Gamma_{\mathrm{t}} M^{-1} f - \mu m g \Gamma_{\mathrm{t}} M^{-1} \Gamma_{\mathrm{t}}^{T}\,] \\ 2\,\mu\, m\, g \end{pmatrix} .$$

The results reported in Figure 2 show the numerically obtained solution is consistent with the analytical solution. Although this is a very simple problem, it is important to note that our solver automatically determines the transition from sliding to rolling at 0.0114 seconds. If the starting conditions were to correspond to rolling contact (with the same end conditions), or if the end conditions had corresponded to sliding contact (with the same starting conditions), the solver would have reported a solution without any transitions. We now turn our attention to a three-dimensional problem of rolling and sliding of a spherical ball on a horizontal plane. It is useful to think of the game of pool or billiards where it is often necessary to deliver the appropriate starting condition to a ball with a desired end condition, a great example of a two-point boundary value problem. The generalized coordinates are $q = [x, y, z, e_0, e_x, e_y, e_z]^T$ and the system velocities are $\nu = [\nu_x, \nu_y, \nu_z, \omega_x, \omega_y, \omega_z]^T$, where $(x,\, y,\, z)$ are the Cartesian coordinates of the center of mass, $(e_0,\, e_x,\, e_y,\, e_z)$

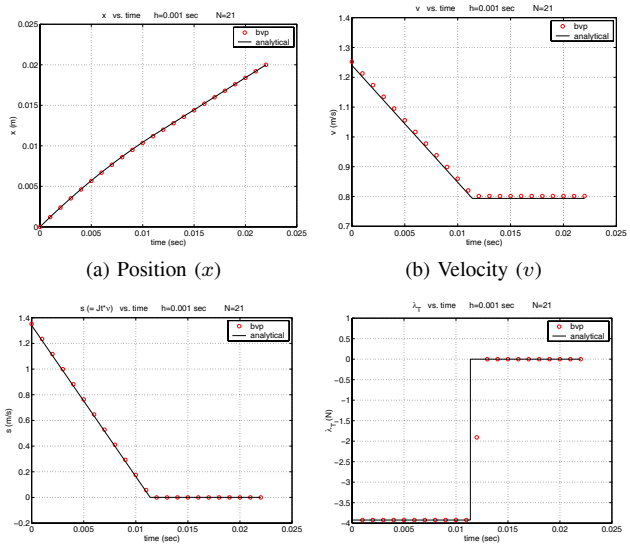

(a) Position (x) (b) Velocity (v)

(c) Relative Velocity (s) (d) Friction force (λ_{t})

Fig. 2. Comparisons between the analytical solutions (solid line) and the numerical solutions from solving the BVP ($N = 21$, time points denoted by circles) with the point of transition being *automatically* established.

are the Euler parameters, $(\nu_x,\, \nu_y,\, \nu_z)$ are the linear velocities along the Cartesian axes, and $(\omega_x,\, \omega_y,\, \omega_z)$ are the angular velocities. Equation (1) is written for a ball of mass m and radius r with

$$G(q) = \begin{bmatrix} 1 & 0 & 0 & 0 & 0 & 0 \\ 0 & 1 & 0 & 0 & 0 & 0 \\ 0 & 0 & 1 & 0 & 0 & 0 \\ 0 & 0 & 0 & -\frac{1}{2}q_5 & -\frac{1}{2}q_6 & -\frac{1}{2}q_7 \\ 0 & 0 & 0 & \frac{1}{2}q_4 & \frac{1}{2}q_7 & -\frac{1}{2}q_6 \\ 0 & 0 & 0 & -\frac{1}{2}q_7 & \frac{1}{2}q_4 & \frac{1}{2}q_5 \\ 0 & 0 & 0 & \frac{1}{2}q_6 & -\frac{1}{2}q_5 & \frac{1}{2}q_4 \end{bmatrix} ,$$

$$f(t, q, \nu) = \begin{bmatrix} 0 & 0 & -mg & 0 & 0 & 0 \end{bmatrix}^T ,$$

$$\Gamma_{\mathrm{n}}(q) = \begin{bmatrix} 0 & 0 & 1 & 0 & 0 & 0 \end{bmatrix}^T ,$$

$$\Gamma_{\mathrm{t}}(q) = \begin{bmatrix} 1 & 0 & 0 & 0 & -r & 0 \end{bmatrix}^T ,$$

$$\Gamma_{\mathrm{o}}(q) = \begin{bmatrix} 0 & 1 & 0 & r & 0 & 0 \end{bmatrix}^T ,$$

and

$$\Psi_{\mathrm{n}}(q^{\ell+1}) = q^{\ell+1}(3) - r.$$

We will use the following parameters for numerical results:

$$n_c = 1, \quad n_q = 7, \quad n_\nu = 6, \quad \mu = 0.2, \quad r = 0.05m,$$
$$m = 0.2Kg, \quad g = 9.8m/sec^2, \quad \gamma = 10^{-4},$$
$$T = 1sec, \quad N = 100, \quad K = 10^4 \cdot I_{3\times 3} N/m.$$

Before solving the boundary value problem we will first solve the initial value problem to illustrate the benefits of the time-stepping model developed here, comparing it to the solutions obtained by the traditional approach involving a rigid

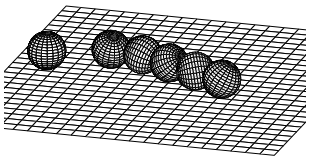

(a) Curved trajectory obtained by striking a pool ball with *english* causing it to exhibit a phenomenon called *massè*

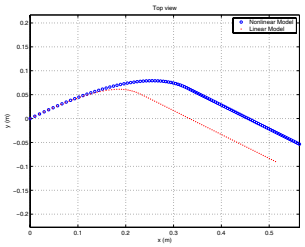

(b) X-Y motion trajectories (circle line denotes the solution to the NCP model (10), dotted line denotes solution by solving the approximate, LCP model).

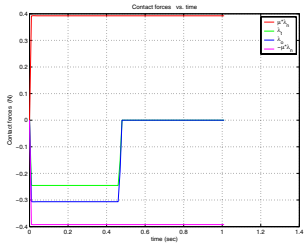

(c) Contact forces (NCP solution).

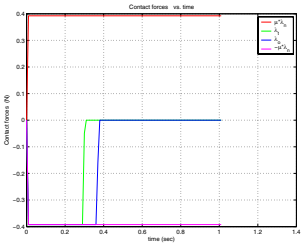

(d) Contact forces (LCP approximation).

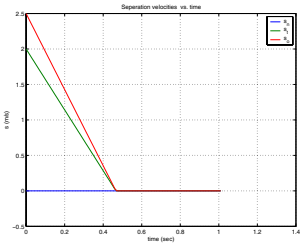

(e) Relative velocities between the ball and the table (NCP solution).

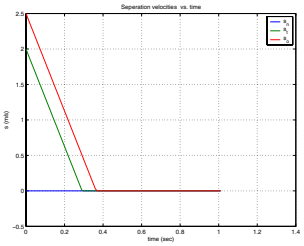

(f) Relative velocities between the ball and the table (LCP approximation).

Fig. 3. Solution to the initial and boundary value problem using fully implicit, rigid-body model with $N = 100$ and $h = 0.01sec$.

body model with a linear friction-pyramid model for frictional forces [14]. In Figure 3, the ball is launched from the origin with a forward initial velocity with back-spin. The initial conditions are:

$$q^0 = [0\ 0\ 0\ 1\ 0\ 0\ 0]^T\,,\ \nu^0 = [1\ 0.5\ 0\ 40\ \ -20\ \ -10]^T\,.$$

We use the PATH solver with AMPL interface to solve the fully implicit, time-stepping compliant model (10) iteratively from $\ell = 0, \ldots, N-1$. The results are shown in Figure 3. The solutions to the NCP compliant model (10) and the more traditional rigid body dynamic model (LCP model in which the Coulomb's friction cone is approximated by a friction pyramid) are compared. We notice that there are some obvious discrepancies between the solutions obtained from the linear model and the complete, nonlinear model. This shows that the pyramid friction law used in the LCP model is a very coarse approximation of the quadratic friction cone. Panels (b-d) illustrates the differences in the trajectory and the contact forces. Panel (f) shows that there are two distinct transitions from sliding to rolling for the LCP approximation – one for the t direction (0.30 seconds) and the other for the o direction (0.37 seconds). This is because the pyramidal approximation decomposes the relative sliding velocity variable into two independent variables, allowing two different sliding velocities.

We now consider the boundary value problem in which we would like to derive initial velocities at a given initial position so that the object reaches a specified position at a specified $time = T$. To plan a feasible motion trajectory for the ball, we need to solve a boundary value problem. As a first check, we can set all the boundary conditions to be consistent with the trajectory generated by the initial value problem. These boundary conditions are shown below:

q^0	q^{N+1}	ν^0	ν^{N+1}
$x^0\ (var.)$	$x^0 + 0.5632$	$v_x^0\ (var.)$	$r\,\omega_y^{N+1}$
$y^0\ (var.)$	$y^0 - 0.0534$	$v_y^0\ (var.)$	$-r\,\omega_x^{N+1}$
0	$z^{N+1}\ (var.)$	0	$v_z^{N+1}\ (var.)$
1	$e_0^{N+1}\ (var.)$	40	$\omega_x^{N+1}\ (var.)$
0	$e_x^{N+1}\ (var.)$	-20	$\omega_y^{N+1}\ (var.)$
0	$e_y^{N+1}\ (var.)$	-10	$\omega_z^{N+1}\ (var.)$
0	$e_z^{N+1}\ (var.)$		

with var denoting the variables that are unspecified. Notice there are a total of 12 unspecified (and 12 specified) boundary conditions, exactly the same number as in the initial value problem and the specified boundary conditions are consistent with the trajectory in Figure 3. The main goal is to determine the initial linear velocities in the x and y directions by solving the boundary value problem. With $N = 100$ time steps, the total number of variables for the boundary value problem is 2300. It takes PATH less than 2 seconds to solve for the complete trajectory. The result is not shown here because it is identical to the result obtained by solving the initial value problem in Figure 3!

In our second example, the traversal of the ball is specified to be $1m$ in the x direction and $-0.1m$ in the y direction, but otherwise it is unchanged from the the previous example. Thus the x and y components of q^{N+1} are set to $x^0 + 1$

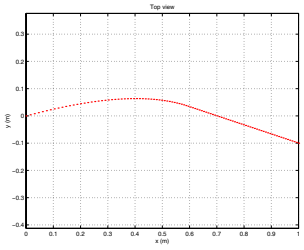

(a) Top view of the motion history

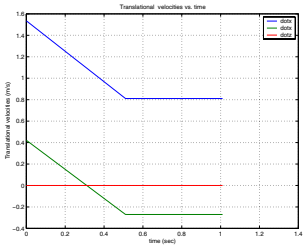

(b) Linear velocities

Fig. 4. Solution to the boundary value problem using the NCP, compliant model (10) to place the object at $(x,\ y) = (1,\ -0.1)$ at $T = 1sec$.

and $y^0 - 0.1$. From Figure 4 (a) it is clear the trajectory satisfies the boundary conditions, and from (b) it is evident that this trajectory requires a higher initial speed because of the increase in distance traverse as compared to the previous example.

B. Transitions from no contact to contact

In addition to transitions between rolling and sliding, transitions from no contact to contact are frequent in manipulation and assembly tasks. These transitions are generally characterized by impacts. In this example, we use the nonlinear, compliant model (10) to solve a boundary value problem involving multiple impacts. The task is to launch the ball from an initial position of $(x,\ y) = (0,\ 0.6)$ to a final position of $(x,\ y) = (0.4,\ 0.4)$ at time $T = 0.45sec$. The boundary conditions for this task are given in the table below.

q^0	q^{N+1}	ν^0	ν^{N+1}
0	0.4	$v_x^0\ (var.)$	$v_x^{N+1}\ (var.)$
0	$y^{N+1}\ (var.)$	0	$v_y^{N+1}\ (var.)$
0.6	0.4	$v_z^0\ (var.)$	$v_z^{N+1}\ (var.)$
0	$e_0^{N+1}\ (var.)$	0	$\omega_x^{N+1}\ (var.)$
0	$e_x^{N+1}\ (var.)$	0	$\omega_y^{N+1}\ (var.)$
0	$e_y^{N+1}\ (var.)$	0	$\omega_z^{N+1}\ (var.)$
0	$e_z^{N+1}\ (var.)$		

Note that these problems are not guaranteed to have unique solutions — for the given initial conditions, there are two classes of solutions to the model (10), one without impacts and one with impacts. The results reported in Figure 5 were obtained by setting $v_z^0 \leq 0$.

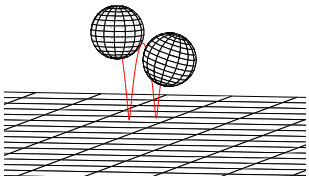

(a) A dynamic trajectory that satisfies the boundary conditions.

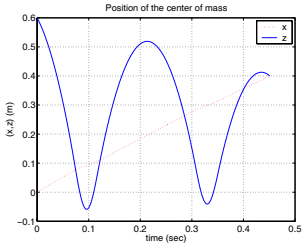

(b) Trajectories of center of mass.

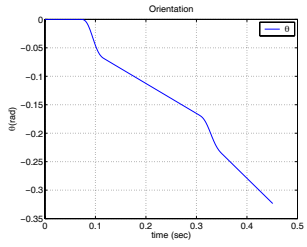

(c) Rotation caused by the frictional impacts.

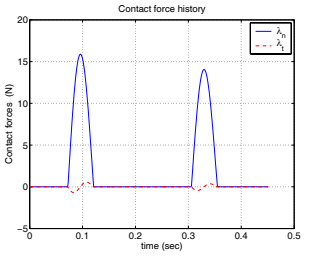

(d) Histories of the contact forces.

Fig. 5. Solution to the boundary value problem for systems involving frictional impacts using the nonlinear, compliant model (10).

C. Reorienting an object for manipulation or part feeding

We now consider a manipulation problem in which we want to reorient a rectangular object of given dimensions, mass, and moment of inertia. For example, it may be necessary to change the orientation of a grasped object by 180 degrees without regrasping. In manufacturing systems one sees part feeders that are able to reorient parts so they always emerge in the same orientation regardless of the incoming pose. One design goal may be to determine the design parameters of the part feeder such that a part entering with different orientations always exits in the orientation with the center of gravity vertically above the geometric center.

Figure 6 shows a simplified part reorienting mechanism with 2 design parameters, (x_p, y_p), the coordinates of the upper-left corner the protrusion which may be the thumb of a hand or a tab in a part-feeder positioned for reorienting the part. The design parameters influence the resulting trajectory which in turn is required to satisfy boundary conditions in the starting and initial position. This problem can be posed as a constrained optimization problem [1] by minimizing a cost function over the design space specified by simple bounds placed on the design variables. Instead of exactly specifying the desired boundary conditions, it is beneficial to impose bounds on the terminal conditions and penalize, via the cost function, the discrepancy between the desired boundary conditions and the boundary conditions obtained from solving the boundary value problem.

In our example, a feasible design was obtained after approximately 1000 objective function evaluations and each one of the evaluations requires solving an initial value problem. We show two sets of results in Figure 6. In (a), we show the results of an initial value problem with $(x_p,\ y_p) = (5,\ 5)$ with the object released from a frictionless chute (which could be replaced by a palm), from a state of rest in the top left corner. The palm is center at $(3.2,\ 0)$. In (b), the results of the two-point boundary-value design problem are shown. The initial conditions of the part is set to the states of the part right after it leaves the input chute. Since there are two design variables, in addition to the initial conditions of the part, we can fix two more boundary conditions. The palm is moved to the left at $(1.7,\ 0)$. In order to accommodate the change of the terminal location, we set the final coordinate of the center of mass at $(x^N,\ y^N) = (2.5,\ 2.1)$ with the final orientation bounded as $0 \leq \theta^N \leq \pi/2$. The constraints on the design variables are

$$4.75 \leq x_p \leq 5.25 \ \text{ and } \ 4.75 \leq y_p \leq 5.25\,.$$

The NCP compliant model (10) was solved by using the PATH solver running on a Linux PC with a 3GHz P4 processor. The solution for the design parameters was found to be $(x_p,\ y_p) = (4.9322,\ 5.1123)$. A fixed time step of $h = 0.001$sec was used. The total number of time steps is $N = 1500$. It takes about 2 to 3 seconds to solve for the design parameters and the complete motion and force history.

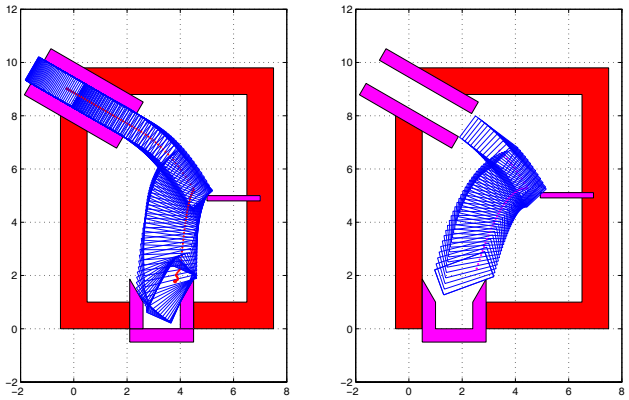

(a) Simulation by solving the initial value problem with an inelastic impact model

(b) Design of the location of the protrusion $(x_p,\ y_p)$ by solving the NCP compliant model.

Fig. 6. A part reorienting design problem with two design variables.

V. Conclusion

We formulated the problem of planning manipulation tasks, which must necessarily involve contact state transitions, as a constrained optimization problem involving boundary conditions at both ends. The discrete-time, nonlinear complementarity problem model described in this paper provides a unified formulation that incorporates intermittent contacts, inelastic and elastic impacts, and transitions between rolling and sliding. To our knowledge, this is the only existing model that allows us to pose the trajectory generation problem for systems with contact state transitions and impacts as a boundary value problem.

The difficulties encountered in this paper arise primarily in the presence of impacts. When impacts occur, the high stiffness associated with the contact compliance leads to stiffness in the equations so that the equations are not well conditioned. The solution at mesh points with finite forces is well conditioned but at mesh points during impact the equations are (locally) stiff. Thus, unlike the examples shown in Figures 2-5 for which the solutions were obtained relatively easily, the example in Figure 6 suffered from problems with convergence because the many potential contact configurations increase the stiffness of this problem. It is possible to to solve a problem with more design variables such as the one considered in our earlier work in [1]. One possibility is to use a shooting method, similar to the approach described in [22], to solve the boundary value problems with estimated parameters and initial conditions. We may still need to rely on the unified model to deal with the discontinuities caused by the contact state transitions. Our ultimate goal is to use the time-stepping models at different levels of resolution and fidelity to solve for trajectories for robotic manipulation iteratively.

Acknowledgement

The authors thank Michael Ferris for providing and supporting PATH and Todd Munson for his help on improving the AMPL/PATH input for the NCP model (10). We gratefully acknowledge support from NSF Grants DMS-0139715 and IIS-0413138.

References

[1] P. Song, J. Trinkle, V. Kumar, and J.-S. Pang, "Design of part feeding and assembly processes with dynamics," in *Proceedings, IEEE International Conference on Robotics and Automation*, May 2004, pp. 39–44.

[2] G. Boothroyd and A. Redford, *Mechanized Assembly: Fundamentals of Parts Feeding, Orientation, and Mechanized Assembly*. McGraw-Hill, 1968.

[3] S. Akella, W. Huang, K. Lynch, and M. Mason, "Sensorless parts feeding with a one joint robot," in *Workshop on the Algorithmic Foundations of Robotics*, 1996.

[4] N. Zumel and M. Erdmann, "Nonprehensible two palm manipulation with non-equilbrium transitions between stable states," in *Proceedings, IEEE International Conference on Robotics and Automation*, April 1996, pp. 3317–3323.

[5] J. D. Wolter and J. Trinkle, "Automatic selection of fixture points for frictionless assemblies," in *Proceedings, IEEE International Conference on Robotics and Automation*, vol. 1, May 1994, pp. 528–534.

[6] T. Zhang and K. Goldberg, "Gripper point contacts for part alignment," *ieee-tra*, vol. 18, no. 6, pp. 902–910, 2002.

[7] M. Cherif and K. Gupta, "Planning quasi-static motions for reconfiguring objects with a multi-fingered robotic hand," in *Proceedings, IEEE International Conference on Robotics and Automation*, April 1997.

[8] G. A. S. Pereira, A. Das, V. Kumar, and M. F. M. Campos, "Decentralized motion planning for multiple robots subject to sensing an d communication constraints," in *Multi-Robot Systems: From Swarms to Intelligent Automata, Volume II*, A. Schultz, L. E. Parker, and F. Schneider, Eds. Kluwer Academic Press, 2003, pp. 267–278.

[9] W. S. Howard and V. Kumar, "On the stability of grasped objects," *IEEE Transactions on Robotics and Automation*, vol. 12, no. 6, pp. 904–917, December 1996.

[10] P. Song, P. Kraus, V. Kumar, and P. Dupont, "Analysis of rigid–body dynamic models for simulation of systems with frictional contacts," *ASME Journal of Applied Mechanics*, vol. 68, pp. 118–128, 2001.

[11] Y. Wang and V. Kumar, "Simulation of mechanical systems with unilateral constraints," *Journal of Mechanical Design*, pp. 571–580, June 1994.

[12] C. Ullrich and D. K. Pai, "Contact response maps for real time dynamic simulation," in *Proceedings, IEEE International Conference on Robotics and Automation*, 1998, pp. 1950–1957.

[13] P. Song, J.-S. Pang, and V. Kumar, "A semi-implicit time-stepping model for frictional compliant contact problems," *International Journal for Numerical Methods in Engineering*, vol. 60, pp. 2231–2261, 2004.

[14] J. Trinkle, J. Pang, S. Sudarsky, and G. Lo, "On dynamic multi-rigid-body contact problems with coulomb friction," *Zeitschrift für Angewandte Mathematik und Mechanik*, vol. 77, no. 4, pp. 267–279, 1997.

[15] D. Baraff, "Fast contact force computation for nonpenetrating rigid bodies," in *Proceedings, SIGGRAPH*, July 1994, pp. 23–34.

[16] B. Mirtich, "Impulse-based dynamic simulation of rigid body systems," Ph.D. dissertation, University of California, Berkeley, The Computer Science Division, 1996.

[17] P. Lötstedt, "Coulomb friction in two-dimensional rigid body systems," *Zeitschrift für Angewandte Mathematik und Mechanik*, vol. Bd.61, pp. 605–615, 1981.

[18] J. Pang, V. Kumar, and P. Song, "Convergence of time-stepping methods for initial and boundary value frictional compliant contact problems," 2004, sIAM Journal on Numerical Analysis.

[19] M. S. Bazaraa and C. M. Shetty, *Nonlinear Programming: Theory and Algorithms*. New York: John Wiley & Sons, 1979.

[20] D. Stewart and J. Trinkle, "An implicit time-stepping scheme for rigid body dynamics with inelastic collisions and coulomb friction," *International Journal of Numerical Methods in Engineering*, vol. 39, pp. 2673–2691, 1996.

[21] M. Anitescu and F. Potra, "Formulating multi-rigid-body contact problems with friction as solvable linear complementarity problems," *ASME Journal of Nonlinear Dynamics*, vol. 14, pp. 231–247, 1997.

[22] J. Popović, S. M. Seitz, M. Erdmann, Z. Popović, and A. Witkin, "Interactive manipulation of rigid body simulations," in *Proceedings of SIGGRAPH 2000*, 2000, pp. 209–218.